International Journal of Radiation Oncology biology • physics

www.redjournal.org

Physics Contribution

4π Noncoplanar Stereotactic Body Radiation Therapy for Centrally Located or Larger Lung Tumors

Peng Dong, PhD,* Percy Lee, MD,* Dan Ruan, PhD,* Troy Long, BS,† Edwin Romeijn, PhD,† Daniel A. Low, PhD,* Patrick Kupelian, MD,* John Abraham, BS,* Yingli Yang, PhD,* and Ke Sheng, PhD*

**Department of Radiation Oncology, University of California Los Angeles, Los Angeles, California; and †Department of Industrial and Operations Engineering, University of Michigan, Ann Arbor, Michigan*

Received Dec 19, 2012, and in revised form Jan 16, 2013. Accepted for publication Feb 2, 2013

Summary

Stereotactic body radiation therapy to centrally located or larger lung tumor results in higher toxicities. To overcome this challenge, we implemented a system that automatically selected and optimized noncoplanar beams. As a result, the dose conformality was significantly improved. Doses to heart, esophagus, trachea/bronchus tree, spinal cord, and lungs were markedly reduced. The improved dosimetry would allow a planning target volume dose escalation from 50 to 68 Gy or higher to these tumors without exceeding critical organ dose limits.

Purpose: To investigate the dosimetric improvements in stereotactic body radiation therapy for patients with larger or central lung tumors using a highly noncoplanar 4π planning system.

Methods and Materials: This study involved 12 patients with centrally located or larger lung tumors previously treated with 7- to 9-field static beam intensity modulated radiation therapy to 50 Gy. They were replanned using volumetric modulated arc therapy and 4π plans, in which a column generation method was used to optimize the beam orientation and the fluence map. Maximum doses to the heart, esophagus, trachea/bronchus, and spinal cord, as well as the 50% isodose volume, the lung volumes receiving 20, 10, and 5 Gy were minimized and compared against the clinical plans. A dose escalation study was performed to determine whether a higher prescription dose to the tumor would be achievable using 4π without violating dose limits set by the clinical plans. The deliverability of 4π plans was preliminarily tested.

Results: Using 4π plans, the maximum heart, esophagus, trachea, bronchus and spinal cord doses were reduced by 32%, 72%, 37%, 44%, and 53% ($P \leq .001$), respectively, and R_{50} was reduced by more than 50%. Lung V_{20}, V_{10}, and V_5 were reduced by 64%, 53%, and 32% ($P \leq .001$), respectively. The improved sparing of organs at risk was achieved while also improving planning target volume (PTV) coverage. The minimal PTV doses were increased by the 4π plans by 12% ($P = .002$). Consequently, escalated PTV doses of 68 to 70 Gy were achieved in all patients.

Conclusions: We have shown that there is a large potential for plan quality improvement and dose escalation for patients with larger or centrally located lung tumors using noncoplanar beams with sufficient quality and quantity. Compared against the clinical volumetric modulated arc therapy and static intensity modulated radiation therapy plans, the 4π plans yielded significantly and consistently improved tumor coverage and critical organ sparing. Given the known challenges in central structure dose constraints in stereotactic body radiation therapy to the lung, 4π planning may increase efficacy and reduce toxicity. © 2013 Elsevier Inc.

Reprint requests to: Ke Sheng, PhD, Department of Radiation Oncology, University of California, Los Angeles, Los Angeles, CA 90095. Tel: (310) 853-1533; E-mail: ksheng@mednet.ucla.edu

Conflict of interest: none.

Int J Radiation Oncol Biol Phys, Vol. 86, No. 3, pp. 407–413, 2013
0360-3016/$ - see front matter
http://dx.doi.org/10.1016/j.ijrobp.2013.02.002

Introduction

Stereotactic body radiation therapy (SBRT) using highly hypofractionated doses, typically 50 to 60 Gy in 3 to 5 fractions, has achieved remarkable success in treating early-stage lung cancer. Excellent local control rates and low toxicity were reported in many clinical trials (1, 2) for non-small cell lung cancer. For early-stage and peripheral lung cancer, SBRT has become the standard of care for medically inoperable early-stage lung cancer with comparable survival rates to those of surgery (1). However, it has also been realized that local control rates decrease with increasing tumor sizes. Dunlap et al reported 90% and 70% local control rates for T1 and T2 tumors, respectively, showing a significant size factor in lung SBRT efficacy (3). Similarly decreased local control rates were observed by other investigators (1, 4). Beitler et al (5) showed much poorer outcomes for gross tumor volume larger than 65 cm^3, roughly the volume dividing stage IA and stage IB lung tumors. Larger treatment volumes also lead to higher doses to organs at risk (OARs). Limited normal organ tolerance not only prevents higher doses from being delivered to larger tumors but also demands compromised, lower prescription doses in practice, further reducing local control rates. Another challenge in lung SBRT has come from treating centrally located lung tumors. Timmerman et al (6) reported an increase of 8- to 10-fold in toxicity compared with peripheral tumors from lung SBRT and associated the toxicity to high doses to central organs with serial radiobiology characteristics. Song et al (7) concluded that SBRT should not be given to centrally located tumors because of the significantly higher probability of severe side effects. However, based on the radiation therapy oncology group (RTOG) central tumor definition of a 2-cm volume around segmental bronchi for central tumors, these constitute a significant number of tumors in which an improvement in sparing of OARs is meaningful. In practice, moderate SBRT doses such as 50 Gy in 4 to 5 fractions, as opposed to 54 to 60 Gy in 3 fractions to peripheral lung tumors, are recommended for these tumors that are larger, centrally located, or both to achieve a balance between local control and normal tissue toxicity (8). The compromise has diminished potential gains in tumor control probability for these tumors because of the significantly lower biological equivalent doses (9).

The RTOG lung SBRT protocol 0813 for centrally located lung tumors (10) constrains the maximum esophagus heart, great vessels, and trachea/bronchus doses to between 18 and 32 Gy, corresponding to approximately 30% to 60% of the prescription doses. The RTOG protocols recommend using either noncoplanar static or coplanar arc beams to achieve the R_{50} dosimetric goal, which is defined as the 50% prescription dose volume divided by the planning target volume (PTV). Lim et al (11) showed that when compared against coplanar plans, a lower R_{50} could be achieved in 81% of patients when noncoplanar beam arrangements were used. However, Christian et al (12) found no dosimetric improvements when comparing noncoplanar and coplanar IMRT plans and that the noncoplanar plan quality was highly dependent on the dosimetrists' experience and the plans were more difficult to deliver.

We previously showed in liver SBRT (13) that large dosimetric gains could be achieved using optimized noncoplanar IMRT beams when compared against state-of-the-art VMAT plans. In the current study, we applied a modified version of the method to these challenging lung SBRT cases to test whether significant dosimetric gains could be achieved, allowing simultaneous critical organ dose reduction and PTV dose escalation.

Methods and Materials

Dose matrix calculation

The planning process began by distributing 1162 noncoplanar candidate beams throughout the entire 4π solid angle space with 6° of separation between 2 nearest neighbor beam pairs. From the candidate pool, we eliminated those beams that would cause collisions between the gantry and the couch or patient. Collisions were determined using a precise computer-assisted design models of the linear accelerator (Varian EX) and a human subject and simulating their relative positions for each candidate beam. The computer-assisted design model was constructed by digitizing the room and patient geometry using a high-precision 3-dimensional (3D) camera (Artec MH). In the retrospective study, 1 human subject 3D model was used to model collisions for all 12 patients, but for future prospective studies, the solution space will be personalized on the basis of individual patient surface topology as measured with 3D optical scanning.

The remaining beams were subdivided into 6×6 mm^2 beamlets, and the dose distribution matrices of each beamlet were calculated with an in-house collapsed-cone convolution/superposition code using 6-MV x-ray polyenergetic kernels and heterogeneity corrections. The dose calculation was matched to 6-MV machine commissioning data. The dose calculation resolution was $3 \times 3 \times 3$ mm^3.

4π optimization

The algorithmic details and validation results of the optimization modeling have been previously introduced (14). A brief review follows here.

We let D_{bk} denote the dose delivered to a voxel from beamlet $k \in K_b$ in beam angle $b \in B$ and $F(z)$ the objective function associated with dose distribution z. The optimization problem is then formulated as follows:

minimize $F(z)$

$$\text{s.t.} \begin{cases} \overrightarrow{z} = \sum_{b \in B'} \sum_{k \in K_b} D_{bk} x_{bk}, & x_{bk} \geq 0, \\ x_{bk} = 0, & b \in B \setminus B',\ k \in K_b \\ & \overrightarrow{z} \leq \overrightarrow{q} \end{cases} \tag{1}$$

where K_b is the set of beamlets at beam angle b, B' represents selected beam orientation sets, $\overrightarrow{z}$ is the 3D dose distribution, and $\overrightarrow{q}$ is the 3D dose constraint. The optimization started from an empty solution set, and for each iteration, a new beam from the remainder of the candidate conformal beam pool $B \setminus B'$ was added to the selected beam set. The beam orientation optimization the fluence map optimization problems were subsequently solved. Beams were added in an iterative process until the desired number of beams was reached or the objective function plateaued. We used an objective function $F(z)$ based on a linear approximation of EUD (15).

$$\begin{cases} F(\overrightarrow{z}) = \sum_m \alpha_m G_m(\overrightarrow{z}) \ \ m \in r, s, r_{50}, V_{20}, V_{10}, V_5, \alpha_m \geq 0 \\ Gr(\overrightarrow{z}) = mean(\max(prescriptiondose - \overrightarrow{z}, 0)).\ for\ PTVr \\ Gs(\overrightarrow{z}) = \gamma_s mean(\overrightarrow{z}) + (1 - \gamma_s)\max(\overrightarrow{z})\ for\ OARs\ \gamma_s \leq 1 \\ Gr_{50}(\overrightarrow{z}) = \gamma_{r_{50}} mean(\max(\overrightarrow{z} - 0.5 * prescriptiondose, 0)) \\ for\ pseudo\ structures \\ G_{V_{20}}(\overrightarrow{z}) = mean(\max(\overrightarrow{z} - 20, 0))\ for\ Lung \\ G_{V_{10}}(\overrightarrow{z}) = mean(\max(\overrightarrow{z} - 10, 0))\ for\ Lung \\ G_{V_5}(\overrightarrow{z}) = mean(\max(\overrightarrow{z} - 5, 0))\ for\ Lung \end{cases}$$

where G_s, G_r, $G_{r_{50}}$, $G_{V_{20}}$,$G_{V_{10}}$ and G_{V_5} are objective functions for OARs, PTVs, pseudostructures, V_{20}, V_{10}, and V_5. The weights among multiobjectives $\alpha'_m s$ were fine-tuned to reach individual planning objectives. The assignment of a voxel that lay within multiple OARs was assigned for purposes of the objective function calculation to the OAR with greatest optimization priority. For the PTV, we used an objective function that punished only cold spots, voxels receiving doses smaller than the prescription dose. Hot spots (ie, voxels with doses greater than prescription dose) were not included in the objective function; instead, a hard constraint of 120% of the prescription dose was set as the maximum PTV dose. This measure simplified the optimization iteration by focusing on increasing the mean PTV dose that received lower than the prescription dose. Unlike our recently published liver study (13), R_{50} was included in the objective function to explicitly optimize this important parameter. A pseudostructure was created outside the PTV to assist the minimization of R_{50} by minimizing the mean dose to voxels with doses greater than 50% of the prescription dose. The percentages of the lung volumes receiving more than 20 Gy (V_{20}), 10 Gy (V_{10}), and 5 Gy (V_5) were similarly included in the objective function. The additional terms in the objective function did not change its convexity.

To determine the relative dosimetric gain from noncoplanarity, both coplanar and noncoplanar plans were created by use of the identical dose computation algorithm, optimization method, and optimization constraints. R_{50} was plotted against beam numbers. The relative gain was used to guide beam number determination in 4π planning.

Comparison with clinical and VMAT plans

The 4π optimization was evaluated on 12 lung SBRT patients previously treated with 7 to 9 IMRT beams planned on iPlan (Brainlab, Germany) involving 1 to 2 noncoplanar angles selected by the dosimetrists. Eleven of the 12 patients received 50 Gy in 4 fractions, and 1 received 50 Gy in 5 fractions. The dose was computed by the Monte Carlo method with an isotropic resolution of 2.5 mm. The maximum gross tumor diameter, PTV, and lung volumes are shown in Table 1. All patients had tumors that were within 2 cm of 1 or more central organs, including the proximal bronchial trees, heart, or esophagus. Eight patients had a tumor dimension greater than stage IB lung cancer as defined by the American Joint Committee on Cancer. Four patients had a lung tumor dimension greater than 5 cm, which is considered large for lung SBRT purposes. To determine whether the original clinical plans were competent, they were replanned on Eclipse using 2 full VMAT arcs (RapidArc). The VMAT final dose was calculated by the analytical anisotropic algorithm with heterogeneity correction. The dose calculation resolution was 2.5 mm.

The common planning objectives included that 95% of the PTV was covered by 100% of the prescription dose and minimization of the heart, esophagus, spinal cord, trachea/proximal bronchus, and normal lung doses. Initial maximum dose constraints to these organs followed RTOG 0618 but were generally further reduced individually.

Regarding computational performance, all calculations were performed on a personal computer with a 6-core processor clocked at 3.8 GHz, and 2 to 10 hours were used to calculate beamlets depending on the PTV size. For a 9.6-cm^3 PTV (patient 3), the optimization took 20 minutes for 30 beams and 10 minutes for 20 beams. For a 138.5-cm^3 PTV (patient 5), the 30-beam optimization time was 3 hours and the 20-beam optimization time was 1.5 hours. Overall computational time of 4π plans was comparable to mainstream IMRT planning systems.

Dose escalation studies were performed using the noncoplanar plans with the goal of gradually increasing the PTV prescription dose and reoptimizing the plans without exceeding any of the clinically defined OAR doses.

The paired t test was used to perform statistical analysis, and a significance level of $P \leq .05$ (2-tailed) was used.

Results

The 4π algorithm was evaluated for each clinical case according to plans that used up to 30 coplanar and noncoplanar fields. The numbers of beams were selected based on the R_{50} comparison between coplanar and noncoplanar plans of a typical patient (Fig. 1b). With fewer than 10 beams, the difference in R_{50} was insignificant and could be compensated for by using more coplanar beams. This agreed with previous observations (16-18). However, with more than 20 noncoplanar beams, the R_{50} of the noncoplanar plan was 30% less than for the coplanar plan and could no longer be matched by using more coplanar beams. Similar patterns were observed in all patients, with the point of divergence varying between 5 and 10 beams. The 4π platform selected 30 noncoplanar beams whose entrances were typically biased toward the side of the patient containing the tumor. This

Table 1 PTV, prescription doses, and normal lung volume of the 12 lung cancer patients

Patient	GTV diameter (cm)	PTV (cm^3)	Prescription dose (Gy)	Normal lung volume (cm^3)	Within 2 cm of
1	6.10	117.0	50	3832	Bronchus
2	7.72	138.4	50	2145	Bronchus
3	3.05	43.6	50	3435	Heart
4	1.81	9.6	50	2010	Heart
5	6.25	138.5	50	2309	Bronchus
6	3.06	50.7	50	3931	Bronchus
7	7.02	135.0	50	3727	Heart, bronchus
8	2.27	30.6	50	2096	Heart, bronchus
9	4.55	80.3	50	1868	Heart, bronchus
10	6.61	100.3	50	6493	Heart
11	4.82	105.7	50	2636	Heart, bronchus
12	4.69	70.0	50	2872	Heart, bronchus, esophagus

Abbreviations: GTV = gross tumor volume; PTV = planning target volume.

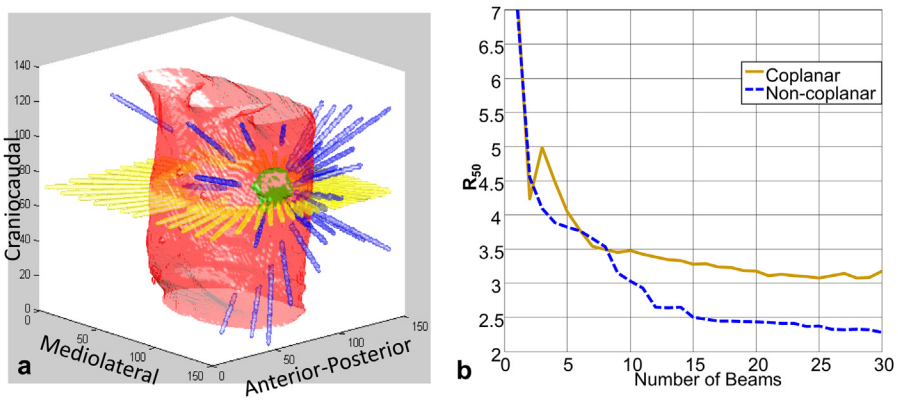

Fig. 1. (a) Optimized noncoplanar (*blue*) and coplanar (*yellow*) beams for a lung cancer patient. (b) R_{50} versus the number of optimized coplanar (*dashed line*) and noncoplanar (*solid*) beams. Color versions of these figures can be found on www.redjournal.org.

formed an irregular conical pattern, as shown in Figure 1a. When constrained to coplanar geometries, the same algorithm selected more evenly distributed coplanar beams. Figure 2 compares the dosimetric quantities, averaged for the 12 cases, that were evaluated in the study. There was no significant difference ($P>.30$) between the clinical static IMRT plans and the VMAT plans, demonstrating equivalence between the coplanar and clinical plans. By contrast, and 4π noncoplanar plans were substantially and significantly better than both clinical plans in every aspect of comparison. Compared against the clinical plan, the maximum doses to the heart, esophagus, trachea, bronchus, and spinal cord were reduced by 32% ($P=.0005$), 72% ($P=.0005$), 37% ($P=.001$), 44% ($P=.0005$), and 53% ($P=.0005$), respectively. V_{20}, V_{10}, and V_5 improved by 64% ($P=.0005$), 53% ($P=.0005$), and 32% ($P=.001$), respectively. R_{50} was reduced by more than 50% for the 4π plans compared against the clinical plans. The superior OAR sparing was achieved with superior PTV minimum dose by 12% ($P=.002$). Dose color wash of a patient (patient 7) with a large posterior left lung tumor is shown in Figure 3 and the dose-volume histogram for the same case is shown in Figure 4.

The improved dose coverage and conformity for the 4π plans afforded the opportunity to escalate tumor dose without compromising OAR sparing. Replanning the 12 cases with the 4π algorithm resulted in 95% PTV coverage by at least 68 Gy (range, 68-70 Gy) for all 12 patients while maintaining the same or lower OAR dose constraints (Fig. 2). The maximum OAR doses increased with the greater prescription doses, but they were still lower than the clinical plans that used the 50-Gy prescription dose. Compared with the clinical plans, the 4π plans improved V_{20}, V_{10}, and V_5 by 36% ($P=.0005$), 33% ($P=.0005$), and 16% ($P=.001$), respectively. Compared with the VMAT plans, the 4π plans improved V_{20}, V_{10}, and V_5 by 23% ($P=.06$), 22% ($P=.0005$), and 33% ($P=.0005$), respectively. Figure 3d shows the dose color wash of the same patient with 70 Gy to 95% of the PTV. Further dose comparison is shown by the dose-volume histogram in Figure 4. Clearly, the 4π plan using 30 noncoplanar beams was markedly superior to the clinical plan with predominantly coplanar beams. The advantage in OAR sparing persisted even when the prescription dose was escalated to 70 Gy.

The deliverability of 4π plans was preliminarily tested using the Varian TrueBeam developer mode. On average, the automated couch and gantry travel added 220 seconds to the beam-on time for 30 noncoplanar beams, which were estimated to have a combined beam-on time of less than 10 minutes using a dose rate of 1000 MU/min for a 12-Gy treatment.

Discussion

It is evident that 4π planning can provide definitive dosimetric improvements to lung SBRT. With 4π radiation therapy, the tumor prescription dose to these patients could be escalated to 68 Gy or higher without exceeding the dose limits set by previous clinical plans, which were well tolerated by these patients. The higher PTV dose has been correlated to significantly higher tumor control probabilities (19, 20), which would be particularly important for larger (stage IB and IIA) and centrally located lung tumors, where the dose conflicts between the normal organ constraints and the PTV could no longer be resolved using

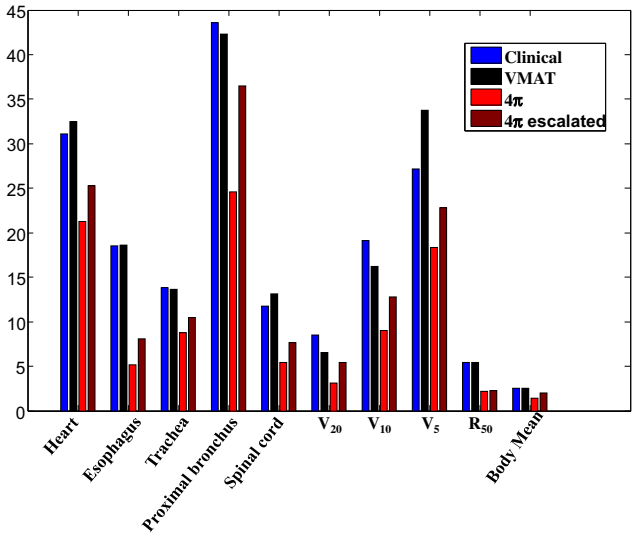

Fig. 2. Collective dosimetric comparison for the 12 patients. The y-axis unit for heart maximum, esophagus maximum, trachea, proximal bronchus maximum, and body mean is Gy; V_{20}, V_{10}, and V_5 are displayed in percentage. R_{50} is unitless. The prescription dose for 4π, clinical 8 fields, and volumetric modulated arc therapy (VMAT) plans is 50 Gy. The prescription dose is 68 to 70 Gy for 4π escalated plans.

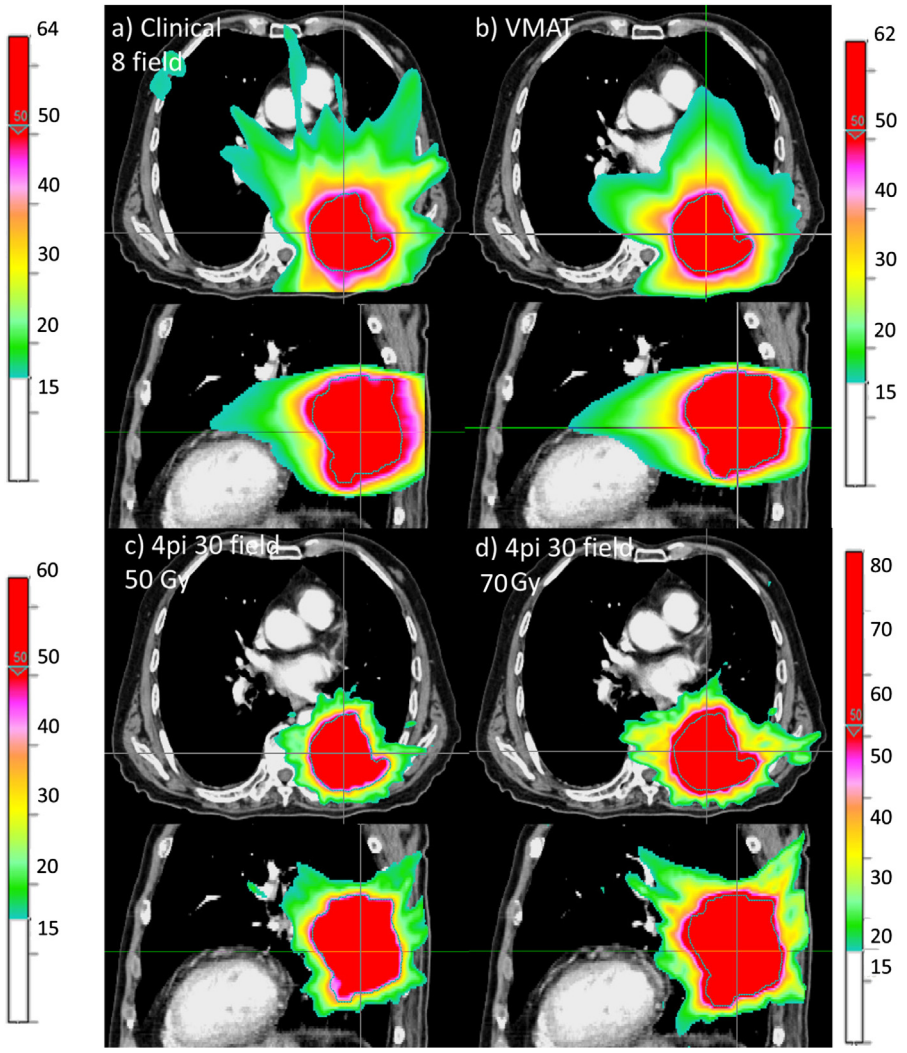

Fig. 3. Dose for 1 patient shown in the axial and sagittal planes: (a) clinical 8-field intensity modulated radiation therapy with 50-Gy prescription dose, (b) volumetric modulated arc therapy (VMAT) plan with 50-Gy prescription dose, (c) 4π 30-field plan with 50-Gy prescription dose, (d) 4π 30-field plan with 70-Gy prescription dose. Notice the different colorbar scale for (d).

coplanar beams and manually selected noncoplanar beams. The biological equivalent dose of 68 Gy delivered in 5 fractions is higher, more so in 4 fractions, than that of 54 Gy in 3 fractions, which was the target dose of RTOG 0618 for >90% local lung tumor control rates.

Previous dosimetric studies using noncoplanar beams on extracranial sites were not conclusive; moderate or mixed gains were reported when noncoplanar beams were used. The equivocal conclusions from the literature, along with the complexity involved in noncoplanar beam planning and delivery, have dampened overall enthusiasm for the extracranial use of the technique. However, the failure to show the definitive usefulness of the noncoplanar technique is due not to the noncoplanar approach but to the limited quality and quantity of noncoplanar beams applied to a clinically practical plan. The lack of mature beam orientation optimization programs operating in the noncoplanar space limits the quality of beam selection. The number of couch kicks in a treatment has been limited to fewer than 10, based on practicality instead of considerations of plan quality. This has put a practical upper boundary on the number of noncoplanar directions in previous planning studies. Although the plan quality does not necessarily benefit from an arbitrarily large number of beams, the point of diminishing returns can be substantially greater than 10 noncoplanar angles. It was shown by a prostate planning study that 25 noncoplanar beams performed significantly better than 10 noncoplanar beams (21). Our data support that more than 10 noncoplanar beams are needed to sufficiently sample the much larger noncoplanar solution space. This can also be intuitively understood from Figure 1a by observing that 30 coplanar beams are crowded but 30 noncoplanar beams are still very sparse. Our study is valuable in elucidating the key elements to the leap in plan quality using 4π planning: quality and quantity of the noncoplanar beams.

The quality of treatment plans is intrinsically affected by the planner experience and the limited number of patients. In our study, the clinical IMRT plans were created by a physicist who specialized in lung SBRT planning and were delivered to patients. The VMAT plans were created by a different dosimetrist, and the results were insignificantly different from the clinical plans. The ranges of planning variation can be estimated from the comparison between the clinical and the VMAT plans

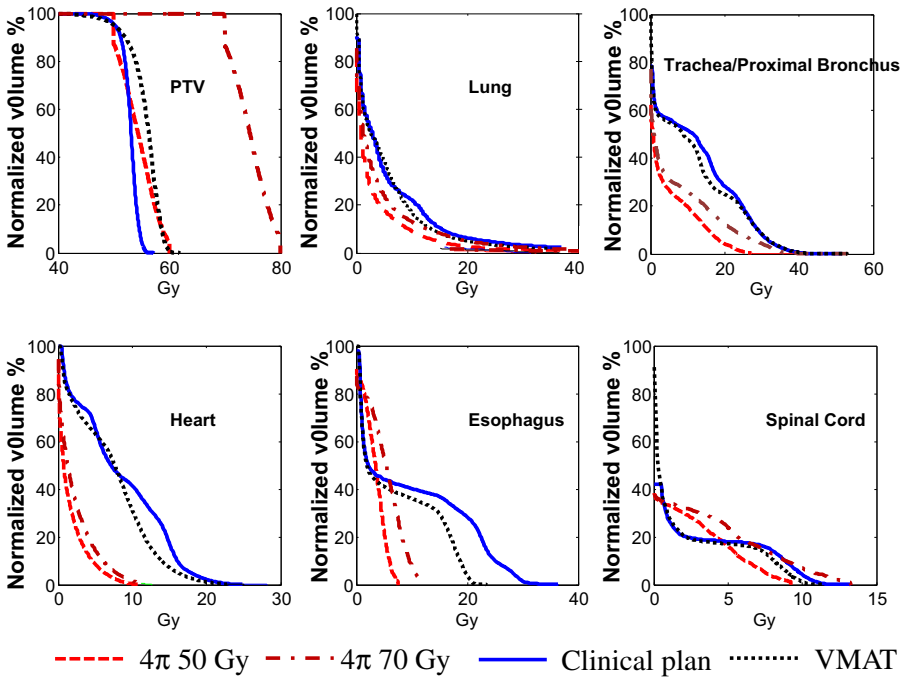

Fig. 4. Dose-volume histogram for the patient shown in Figure 3, red (*dashed*) and brown (*long-short dashed*) lines represent 4π 30-field plan with prescription doses 50 Gy and 70 Gy; blue (*solid*) and black (*dotted*) lines denote clinical 8-field clinical plan and volumetric modulated arc therapy (VMAT) plan with a prescription dose of 50 Gy. PTV = planning target volume.

and were substantially less than the dosimetric improvement from the 4π plans. Another limitation of the study is that 4π plans have not been clinically delivered. Currently, the greatest concerns about using a large number of noncoplanar beams are treatment delivery time and collision avoidance. The maneuvering of couch and gantry between 2 noncoplanar beams could slow down the clinical flow and increase the risk of operator error. This hardware challenge of delivery accuracy and automation has been resolved with a new generation of robotic C-arm linac systems, which were recently introduced by major linac vendors to allow efficient and accurate automatic sequencing from 1 beam angle to another, eliminating a critical hardware limitation to implementing 4π planning and delivery. Our preliminary tests on 1 such system suggest that 4π plan delivery time should not be significantly longer than in the current practice. However, challenges in beam delivery sequence optimization, collision modeling, and prevention need to be addressed before clinical implementation.

Conclusion

A novel treatment planning method has been proposed incorporating beam orientation and fluence map optimization algorithms on the full 4π noncoplanar solid angle space. Algorithm performance was examined by comparing lung SBRT plans for patients with tumors that were larger, centrally located, or both. Compared against state-of-the-art VMAT plans and 7 to 9 static IMRT beams selected by dosimetrists, the 4π plans yielded significantly and consistently superior performance in tumor coverage and in sparing of normal lung and other critical organs. This is fundamentally a result of the dosimetric gains from effective utilization of noncoplanar beam geometry.

References

1. Onishi H, Shirato H, Nagata Y, et al. Stereotactic body radiotherapy (SBRT) for operable stage I non-small-cell lung cancer: Can SBRT be comparable to surgery? *Int J Radiat Oncol Biol Phys* 2011;81:1352-1358.
2. Timmerman R, Paulus R, Galvin J, et al. Stereotactic body radiation therapy for inoperable early stage lung cancer. *JAMA* 2010;303:1070-1076.
3. Dunlap NE, Larner JM, Read PW, et al. Size matters: a comparison of T1 and T2 peripheral non-small-cell lung cancers treated with stereotactic body radiation therapy (SBRT). *J Thorac Cardiovasc Surg* 2010;140:583-589.
4. Fakiris AJ, McGarry RC, Yiannoutsos CT, et al. Stereotactic body radiation therapy for early-stage non-small-cell lung carcinoma: Four-year results of a prospective phase II study. *Int J Radiat Oncol Biol Phys* 2009;75:677-682.
5. Beitler JJ, Badine EA, El-Sayah D, et al. Stereotactic body radiation therapy for nonmetastatic lung cancer: An analysis of 75 patients treated over 5 years. *Int J Radiat Oncol Biol Phys* 2006;65:100-106.
6. Timmerman R, McGarry R, Yiannoutsos C, et al. Excessive toxicity when treating central tumors in a phase II study of stereotactic body radiation therapy for medically inoperable early-stage lung cancer. *J Clin Oncol* 2006;24:4833-4839.
7. Song SY, Choi W, Shin SS, et al. Fractionated stereotactic body radiation therapy for medically inoperable stage I lung cancer adjacent to central large bronchus. *Lung Cancer* 2009;66:89-93.
8. Rowe BP, Boffa DJ, Wilson LD, et al. Stereotactic body radiotherapy for central lung tumors. *J Thorac Oncol* 2012;7:1394-1399.
9. Mehta VK, Lee QT, Chang SD, et al. Image guided stereotactic radiosurgery for lesions in proximity to the anterior visual pathways: A preliminary report. *Technol Cancer Res Treat* 2002;1:173-180.
10. Timmerman R, Kavanagh B. Stereotactic Body Radiation Therapy. Philadelphia: Lippincott Williams & Wilkins; 2004.

11. Derycke S, Van Duyse B, De Gersem W, et al. Non-coplanar beam intensity modulation allows large dose escalation in stage III lung cancer. *Radiother Oncol* 1997;45:253-261.
12. Christian JA, Bedford JL, Webb S, et al. Comparison of inverse-planned three-dimensional conformal radiotherapy and intensity-modulated radiotherapy for non-small-cell lung cancer. *Int J Radiat Oncol Biol Phys* 2007;67:735-741.
13. Dong P, Lee P, Ruan D, et al. 4π Non-coplanar liver SBRT: A novel delivery technique. *Int J Radiat Oncol Biol Phys* 2013 [In press].
14. Romeijn HE, Ahuja RK, Dempsey JF, et al. A column generation approach to radiation therapy treatment planning using aperture modulation. *SIAM J Optim* 2005;15:838-862.
15. Thieke C, Bortfeld T, Kufer KH. Characterization of dose distributions through the max and mean dose concept. *Acta Oncol* 2002;41: 158-161.
16. Hsieh CH, Liu CY, Shueng PW, et al. Comparison of coplanar and noncoplanar intensity-modulated radiation therapy and helical tomotherapy for hepatocellular carcinoma. *Radiat Oncol* 2010;5:40.
17. Holt A, van Vliet-Vroegindeweij C, Mans A, et al. Volumetric-modulated arc therapy for stereotactic body radiotherapy of lung tumors: A comparison with intensity-modulated radiotherapy techniques. *Int J Radiat Oncol Biol Phys* 2011;81:1560-1567.
18. Brock J, Bedford J, Partridge M, et al. Optimising stereotactic body radiotherapy for non-small cell lung cancer with volumetric intensity-modulated arc therapy: A planning study. *Clin Oncol (R Coll Radiol)* 2012;24:68-75.
19. McCammon R, Schefter TE, Gaspar LE, et al. Observation of a dose-control relationship for lung and liver tumors after stereotactic body radiation therapy. *Int J Radiat Oncol Biol Phys* 2009;73:112-118.
20. Onimaru R, Fujino M, Yamazaki K, et al. Steep dose-response relationship for stage I non-small-cell lung cancer using hypofractionated high-dose irradiation by real-time tumor-tracking radiotherapy. *Int J Radiat Oncol Biol Phys* 2008;70:374-381.
21. Rossi L, Breedveld S, Heijmen BJ, et al. On the beam direction search space in computerized non-coplanar beam angle optimization for IMRT-prostate SBRT. *Phys Med Biol* 2012;57:5441-5458.